Improving wear resistance of epoxy resin using bio-oil from hemp biomass: A sound strategy to reduce environmental impact

Journal of Cleaner Production 495 (2025) 145003

Contents lists available at ScienceDirect

Journal of Cleaner Production

journal homepage: www.elsevier.com/locate/jclepro

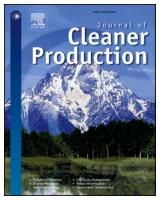

Improving wear resistance of epoxy resin using bio-oil from hemp biomass: A sound strategy to reduce environmental impact

D. Duraccio [a,*], M. Di Maro [a], F. Vaccaro [b], M.G. Faga [a], M. Bartoli [c], G. Malucelli [d], F. Auriemma [e], M. Milazzo [e], O. Ruiz de Ballesteros [e], M. Petrozziello [f], A. Asproudi [f], A. Carpignano [b], R. Gerboni [b]

[a] Istituto di Scienze e Tecnologie per L'Energia e La Mobilità Sostenibili CNR Sede Secondaria Strada Delle Cacce, 73 10135 Torino, Italy
[b] Politecnico di Torino - Dipartimento di Energia Corso Duca Degli Abruzzi 24, 10129 Torino, Italy
[c] Center for Sustainable Future Technologies, Fondazione Istituto Italiano di Tecnologia, Via Livorno 60, 10144 Torino, Italy
[d] Politecnico di Torino - Dipartimento di Scienza Applicata e Tecnologia, Viale Teresa Michel 5, 15121 Alessandria, Italy
[e] Dipartimento di Scienze Chimiche, Università di Napoli Federico II, Complesso Monte S. Angelo, Strada Comunale Cinthia, 26, 80126 Napoli, Italy
[f] Consiglio per La Ricerca in Agricoltura e L'analisi Dell'economia Agraria – Centro di Ricerca per L'Enologia, Via P. Micca 35, Asti, 14100 Italy

ARTICLE INFO

Handling Editor: Dr. Sandra Eksioglu

Keywords:
Hemp hurd
Pyrolysis
Bio-oil
Epoxy resin
Bio-resin
Wear
Crosslink density
Life cycle assessment

ABSTRACT

Efforts are underway to convert biomass into valuable bio-based chemicals, fostering reduced dependence on fossil fuels and advancing sustainability. In this work, various amounts of hemp bio-oil were used to partially replace the amine-based curing agent in a commercial epoxy resin designed for the building sector. All the so-formulated epoxy systems showed a complete degree of curing. The values of crosslinking density decreased to 30% at the highest bio-oil concentration and it was hypothesized that some components of bio-oil reacted with epoxy units acting as dangling groups to resin. These features significantly affected the mechanical properties of the bio-resins: by increasing the amount of bio-oil, the Martens hardness and the indentation Young's modulus decreased (by 20 and 37%, respectively when the bio-oil was half the amount of the amine-based curing agent), while the damping ability of the bio-resin increased. For the commercial resin, the wear track showed an average depth of 86 ± 15 μm and a specific wear rate of 3.62×10^{-4} $mm^3/N{\cdot}m$. These values decreased by 59 and 89%, respectively, when the bio-oil used was half the amount of the amine-based curing agent. The results of the life cycle assessment, including the hemp hurd separation from fibers in the system boundaries, appeared only slightly favorable for the bio-based solutions. However, when also considering the technical life (i.e., wear resistance) of the resins, a significant reduction of all impacts was observed, achieving more than 80% when bio-oil was half the amount of the amine-based curing agent.

1. Introduction

Hemp is a versatile and valuable plant that has been grown and used for thousands of years. Beyond the industrial uses that can be made of its fibers in the textile field, its cultivation offers numerous advantages also from an agronomic point of view. Hemp biomass is a rapidly renewable resource. It is a fast-growing crop in different climates and soil types (Duque Schumacher et al., 2020); it also has a short growing cycle of about 100 days and requires fewer inputs than other crops. Hemp cultivation can be exploited in crop rotation systems to improve soil health, reduce soil erosion, and control weeds naturally (Adesina et al., 2020). Its cultivation requires a minimal amount of pesticides, herbicides, and water compared to many other crops. As a fast-growing crop, it absorbs significant amounts of CO_2 from the atmosphere, contributing to the reduction of greenhouse gases and combating climate change (Finnan and Styles, 2013). Hemp-derived products can serve as a substitute for petroleum-based materials, enabling the development of biodegradable and eco-friendly alternatives in diverse applications. Moreover, hemp bio-oil production does not compete with food supply chains, unlike some biofuels derived from edible crops. This ensures an ethical and sustainable resource allocation. Historically, hemp was widely cultivated in Piedmont, a northwestern region of Italy, for various uses including textiles and ropes. Reviving hemp cultivation can reconnect the region with its agricultural heritage and promote

* Corresponding author.
E-mail address: donatella.duraccio@stems.cnr.it (D. Duraccio).

https://doi.org/10.1016/j.jclepro.2025.145003
Received 9 September 2024; Received in revised form 21 January 2025; Accepted 9 February 2025
Available online 12 February 2025

cultural preservation. To recover the fibers, the hemp stalks are retted by using different approaches, namely: water, dew, enzymatic, and chemical retting. Then, the stalks are mechanically processed to separate the fibers from the hurd (i.e., the coarser and more wood-like part of the stalk), which can be repurposed for various applications such as animal bedding, construction materials, or compost (Duque Schumacher et al., 2020; Zimniewska, 2022).

Recently, efforts have been made to develop value-added products from biomass side streams and waste materials such as different bio-based chemicals able to reduce the reliance on finite fossil resources, contributing to resource conservation and sustainability. The production of renewable chemicals from biomass supports the transition toward a bio-based economy. Among the different methodologies for the valorization of biomass, pyrolysis is one of the most studied due to its versatility, product diversity, waste reduction potential, and climate change mitigation benefits (Kim et al., 2020). Biomass pyrolysis is a thermochemical process in which organic matter (wood, agricultural residues, or other biological materials) is heated in the absence of oxygen (Ning et al., 2013). Anaerobic conditions prevent the complete combustion of biomass and promote the formation of several products, including biochar, gas, and bio-oil. Bio-oil is the liquid fraction of the pyrolysis process and is obtained from the vapor condensation of thermal depolymerization and decomposition of biomass structural components (Ghodake et al., 2021). The composition of pyrolysis oils is highly diversified and strongly depends on the type of biomass used. In particular, more than 200 different compounds are produced by different types of reactions (condensation, hydrolysis, isomerization, and hydrogenation), including carboxylic acids, alcohols, aldehydes, esters, ketones, phenolic and nitrogenous compounds (Balat, 2011). They can be used to obtain various useful products such as fuels (Foong et al., 2021), fertilizers (Ghodake et al., 2021), and raw carbonaceous materials (Kim et al., 2020). Also, bio-oil has been used as a partial substitute in epoxy formulations, to obtain materials with lower toxicity and reduced carbon footprint (Agbo et al., 2023; Baroncini et al., 2016; Pappa et al., 2022).

Epoxy resins are largely used in different industrial products and systems as protective coatings due to their unique combination of properties (Liu et al., 2018; Pulikkalparambil et al., 2018; Zakaria et al., 2015; Zhang et al., 2002; Sharath et al., 2024; Arpitha et al., 2024). However, their production process has a high environmental impact (Pappa et al., 2022) and represents a well-known health risk factor (Bourne et al., 1959). In fact, they contain several components that can be toxic, particularly in their uncured or improperly handled state (Pupin et al., 2017). For these reasons, in the last years, the development and use of environmentally friendly alternatives to hazardous components in epoxy resin formulations have been reported in the literature (Pappa et al., 2022); furthermore, the synthesis of biobased epoxy resins by using lignocellulosic biomass has shown encouraging findings (Auvergne et al., 2014; Baroncini et al., 2016; Celikbag et al., 2017; Koike, 2012; Raquez et al., 2010). The bio-resin should offer comparable functionality to traditional formulations and is likely to represent a more sustainable solution compared with existing fossil-based standard epoxy resins (Pappa et al., 2022). However, the question remains whether these materials are truly more sustainable than those derived from petroleum (Shahid et al., 2024; Kousaalya et al., 2020; Rosenboom et al., 2022; Pascoe Ortiz, 2023; Ares-Elejoste et al., 2023). Assessing sustainability requires a multidisciplinary study and a comprehensive lifecycle analysis, which include also the agricultural process for obtaining the raw biomass.

In this manuscript, for the first time, the feasibility of employing an as-obtained bio-oil derived from pyrolysis of hemp hurd biomass as a partial substitute for amine-curing agents is assessed. The aim is to respond to the need to reduce dependence on limited fossil resources, to promote resource efficiency, and thus to increase sustainability. The environmental impact is also assessed by including, for the first time, the mechanical separation of hurd from hemp fibers. The inclusion of this process ensures a holistic understanding of the material's environmental footprint and offers a more representative and real evaluation of impacts. In particular, different amounts of a bio-oil obtained by the pyrolysis of a hemp hurd side stream were employed as a partial substitute for the amine-based curing agent of a commercial epoxy resin, formulated for construction and lamination in the building sector. The curing ability of the bio-oil was studied using structural analyses (Infrared Spectroscopy, Wide-Angle and Small-angle X-ray Scattering (WAXS, and SAXS)) and swelling tests for measuring the crosslinking density. Also, the mechanical properties and wear resistance of the obtained epoxy systems were investigated. A preliminary assessment of the environmental impacts associated with the new products was carried out and compared with the industrial production process of the epoxy resin. The mechanical separation of hemp hurd from fibers, the production of the bio-oil, and the durability of the prepared bio-resins (in terms of their wear resistance) were also considered in the system boundaries.

2. Materials and methods

2.1. Hemp hurd collection

The raw material used in this work was hurd obtained from a variety of hemp (Cannabis sativa L.) called "Carmagnola" growth and cropped in Piedmont. The hurd was supplied by Assocanapa s. r.l. (the Italian association of hemp producers), which uses a patented prototype (Fig. S1) for the mechanical separation of fibers and hurd from hemp bales, and which could allow for the creation of a short supply chain of secondary hemp products of particular interest (Bartoli et al., 2022; Delmastro, 2010). The machine can process 10 q/h, yielding about 77.5 wt% of hurd, 20 wt% of fibers, and 2.5 wt% of residues. The hurd consisted of chipboards less than 1 cm in length.

2.2. Bio-oil from hemp hurd

2.2.1. Bio-oil preparation – pyrolysis

The thermal decomposition of the recovered hurd took place in a prototype reactor, i.e., a laminar flow tubular kiln (Carbolite TZF 12/65/550), consisting of a horizontal hollow cylinder of 5 cm of diameter and 1 m in length heated by electrical resistances (Bartoli et al., 2022). The hurd was placed in semi-cylindrical steel containers introduced into the reactor. The inert atmosphere was maintained with a nitrogen gas laminar flow of 2.0 L/min. The heating rate applied was 15 °C/min, and the maximum temperature of 500 °C was maintained for 30 min. Bio-oil was collected using a water-cooled condenser system. After cooling down to room temperature without using an external heat exchanger, 24 wt% of bio-oil, 32 wt% of biochar, and 44 wt% of a gaseous mixture of water vapor and carbon dioxide (in a 2:1 ratio) were obtained.

2.2.2. Bio-oil characterization – GC-MS

Volatile compounds were analyzed using an Agilent 6890 gas chromatograph (GC) linked to a 5973 mass spectrometer with a Restek Stabilwax-MS capillary column (30 m × 0.25 mm x 0.25 μm), employing helium as the carrier gas at a constant flow (1.0 ml/min). The temperature program of the GC oven started at 45 °C then increased at a rate of 30 °C/min to 60 °C, where it was held for 2.00 min. The temperature was subsequently raised at a rate of 2 °C/min to 160 °C, followed by a final increase at 30 °C/min to 230 °C. This final temperature was held for 15.00 min to facilitate the elution of higher boiling point compounds. The total runtime of this temperature program was 90.83 min.

The mass spectrometer operated in electron impact (EI) mode, with a 29 to 300 scan range of m/z. Both the MS source and quadrupole temperatures were controlled at 230 °C and 150 °C, respectively. A solvent delay of 5.00 min was incorporated to prevent interference from residual solvents in the analysis of target compounds.

Approximately 1 g of the sample was subjected to solid/liquid extraction using dichloromethane suitable for GC applications

(LiChrosolv® Merck) as the solvent. The extract was then gently treated under a moderate stream of nitrogen to achieve an optimal concentration for analysis. Subsequently, the solution was filtered through a 0.22 μm polytetrafluoroethylene (PTFE) filter to eliminate any particulate matter.

The identification of volatile compounds was conducted by comparing their mass spectra with those in databases integrated into the GC-MS system (NIST v.8 mass spectral library). Additionally, retention times were matched with those of established standards to improve accuracy whenever these standards were available. The objective of the analysis aimed to delineate the overall composition of the extract to provide fundamental insights into its chemical composition.

2.3. Preparation of bio-resins

The epoxy resin (EP commercial) used for this work is Epoxyresins LPL, a commercial product that can be used for construction and lamination in the building sector. It was purchased by Cores S. r.l. And it is a two-component formulation, consisting of diglycidyl ether of bisphenol A (DGEBA) (component A – 5.87 meq/g) and an amine-based curing agent (component B composed by 1,3-phenylenedimethanamine and N1,N3-dimethylpropane-1,3-diamine in 1:1 ratio by weight and catalytic amount of 4-(dimethylamino)-2,6-bis(methylamino)phenol), formulated to have a low viscosity and a long pot life.

A 2:1 epoxy resin/curing agent ratio was employed, as indicated by the resin supplier. For the preparation of bio-resins, component B was partially replaced by bio-oil obtained from the pyrolysis of hurd. The bio-oil/amine ratios adopted are as follows: 1:8, 1:4, 1:2, and 1:1. These ratios were used for coding the bio-resins: for example, EP bio 1:8 indicates the bio-resin, in which the ratio of the bio-oil to the amine curing agent is 1:8.

The cured bio-resins were obtained first by mixing component B with the bio-oil; then, the resulting mixture was added to the epoxy base resin (component A). This whole process was carried out at room temperature. The curing process took place in a furnace at 80 °C for 16 h and then at 110 °C for a further 4 h. A typical sample picture is shown in Fig. S2.

2.4. Structural characterization of the bio-resin

2.4.1. ATR-IR spectroscopy

Attenuated Total Reflection Infrared (ATR-IR) spectra of the bio-resin systems were acquired with a spectrometer Nicolet 5700 (Thermoscientific, Waltham, MA, US) equipped with a diamond window (Smart orbit, Thermoscientific, Waltham, MA, US) in the range between 4000 and 400 cm^{-1}, with a resolution of 2 cm^{-1} and 32 scans. The bio-oil spectrum was also recorded for comparison.

2.4.2. SAXS and WAXS

SAXS and WAXS data of the cured resins have been simultaneously collected at room temperature using a Kratky compact camera "SAXSess" (Anton Paar, Graz, Austria) attached to a conventional X-ray source (Cu Kα radiation, working at wavelength λ = 0.15418 nm). The experiments were carried out in a linear collimation geometry. The scattered radiation was captured on a FUJIFILM BAS-MS Imaging Plate and then processed with a digital imaging reader, specifically the PerkinElmer Cyclone Plus Phosphor Imager (storage phosphor reader). Data were collected within the q range of 0.09–30 nm^{-1}, where q is defined as $4\pi \sin\theta/\lambda$, with 2θ representing the scattering angle. Subsequently, a series of corrections were applied, which included subtraction for dark current, removal of contributions from the empty sample holder, and subtraction of a constant background originating from thermal density fluctuations. Then, for the low q-range region (from 0.09 to ≈1.4 nm^{-1}, the initially collected slit-smeared data were subjected to deconvolution with the primary beam intensity distribution by using the SAXSquant 2.0 software (Anton Paar, Graz, Austria). The outcome of this operation was the calculation of equivalent one-dimensional SAXS profiles that would have been obtained if a point collimation geometry had been employed, essentially achieving the "desmearing" of the data. The scattering data collected in the WAXS region (for q greater than ≈2 nm^{-1}, $2\theta \geq \approx 3°$) was not further reduced and plotted as a function of 2θ.

2.5. Differential scanning calorimetry (DSC)

DSC measurements were performed on 8 mg of samples with a DSC Q2000 (TA instruments, New Castle, DE, USA) working under inert atmosphere (20 ml/min N_2). A heating run from 10 °C to 120 °C with a heating/cooling rate of 10 °C/min was performed to verify the possible occurrence of post-curing effects.

2.6. Swelling test, sol fraction, and crosslinking density evaluation

EP-based resins were cut into square pieces of approximately 15–20 mg (0.6 cm × 0.6 cm). The pieces were weighed and then immersed in 10 ml of methanol (molar volume V_s = 40.45 cm^3/mol; density ρ_s = 0.792 g/cm^3) at room temperature. The samples were placed into glass vials, each equipped with a screw cap assembled with a black phenolic rubber-lined closure to avoid solvent evaporation. During the swelling test, the samples were removed from the solvent, blotted gently with absorbent paper to remove the excess solvent on the surface, and weighed every 10–12 h, until a constant weight was reached (e.g., approximately after 72 h). At the end of the swelling period, the samples were dried in an oven at 55 °C for 48 h and, then, weighed to determine the mass of the dry network after extraction of soluble materials.

The volume fraction of the crosslinked sample at swelling equilibrium (V_r) was calculated according to Eq. (1):

$$V_r = \frac{\frac{W_{dry}}{\rho_{dry}}}{\frac{W_{dry}}{\rho_{dry}} + \frac{W_{sw} - W_{dry}}{\rho_s}} \quad (1)$$

where W_{dry} is the weight of the dry sample, W_{sw} is the weight of the swollen epoxy resin with solvent at equilibrium and ρ_{dry} represents the density of the dry sample.

The crosslinking density ν_e was calculated by the classical Flory-Rehner equation (Flory and Rehner, 1943). This equation assumes that the change of free energy upon swelling is the sum of the change of polymer/solvent mixing free energy and an elastic contribution due to the variation of chain conformation of the network strength. At swelling equilibrium, the sum of these contributions should be zero. For a tetrafunctional affine network, the Flory-Rehner equation is:

$$\nu_e = -\frac{1}{V_s}\frac{\ln(1 - V_r) + V_r + \chi V_r^2}{\sqrt[3]{V_r} - \frac{V_r}{2}} \quad (2)$$

where χ represents the Flory-Huggins polymer-solvent interaction parameter. For the systems epoxy resin/methanol, χ (equal to 1.103) was calculated using the Hansen solubility parameters (Eq. (3)) (Lindvig et al., 2002):

$$\chi = \frac{V_s}{RT}(\delta_s - \delta_p)^2 \quad (3)$$

where δ_s (Brandrup and Immergut, 1975) and δ_p (Li and Strachan, 2018) are the Hansen solubility parameters of the methanol and the DGEBA, respectively and R is the ideal gas constant.

2.7. Mechanical and tribological properties

2.7.1. Dynamic-mechanical tests

The dynamic-mechanical properties of the different bio-resin types were evaluated using a DMA Q800 (TA instruments) apparatus, in dual cantilever configuration. To investigate the viscoelastic behavior of the bio-resins, i.e., the evolution of the storage modulus (E'), loss modulus

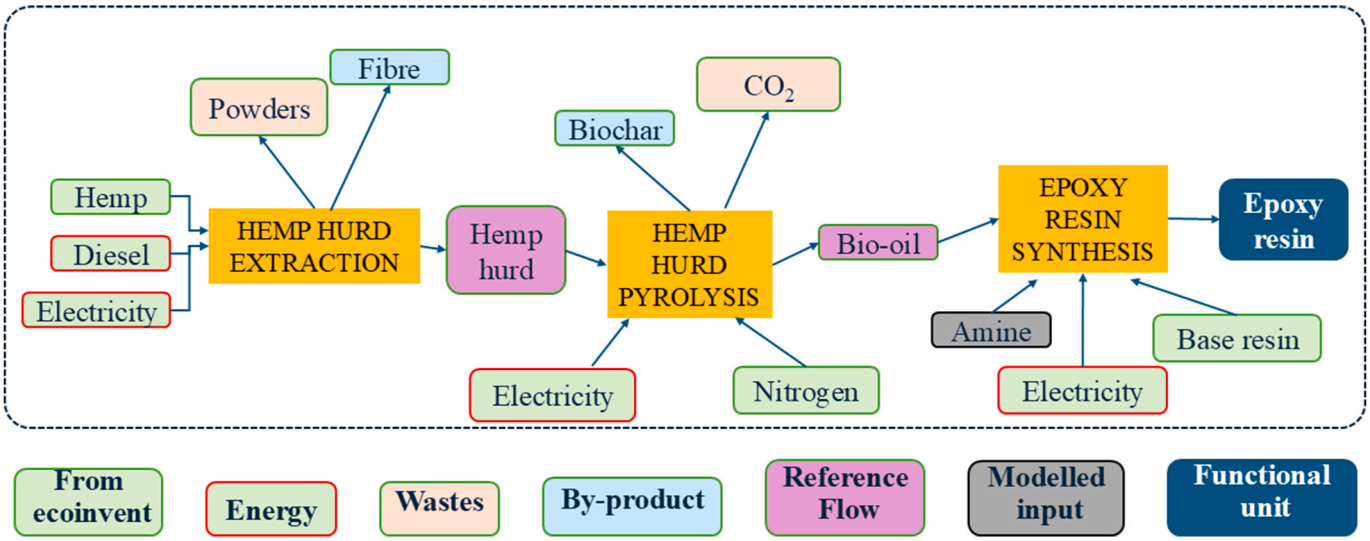

Fig. 1. System boundaries of the modeled epoxy resin production process, from cradle to gate.

(E''), and loss factor (tan δ = E''/E'), dynamic oscillatory tests were performed at a constant frequency of 1 Hz, and 0.05 % strain amplitude. The samples (6.2 mm × 2.8 mm x 8 cm) were subjected to constant heat flow (3 °C/min heating rate) in the range from 30° to 100 °C.

2.7.2. Micro-hardness tests

The hardness (H_m) and the indentation Young's modulus (E_{IT}) of the cured bio-resins were evaluated by micro-hardness tests with a FISCHERSCOPE HM 2000 micro-indenter (Helmut Fischer, Sindelfingen, Germany), equipped with a Vickers indenter. The experiments were performed using a load of 300 mN and a dwell time of 20 s. 10 measurements were performed for each sample.

2.7.3. Ball-on-disk tests

The tribological properties of the cured samples were investigated by a CSEM pin-on-disk tribometer (Alpnach, Switzerland). The evolution of the friction coefficient (COF) as a function of the number of laps was recorded in the ball-on-disc configuration tests. Then, the mean value of three measurements of the steady-state COF was calculated.

Each sample (19 mm × 19 mm x 4.08 mm) was subjected to wear using a 6 mm radius 100 Cr_6 ball. The tests were performed with a normal load of 7 N, for 30,000 laps at a linear speed of 10 cm/s with an operating radius of 5 mm. The tests were carried out at room temperature.

Wear rate was evaluated in according to the Archard's model, described by Eq. (4) (Bhushan, 2013):

$$k_w = \frac{V}{s \cdot N} \tag{4}$$

where V is the wear volume (mm^3), s is the total sliding distance (m) and N is the normal applied load (N). The total sliding distance and the applied load were imposed based on operational conditions; the wear volume was computed by integrating the resulting area evaluated by the profilometry measurements.

2.7.3.1. Profilometry. To calculate the specific wear rate ($mm^3/m \cdot N$) of the various types of resin, the resulting wear traces were analyzed using a contact profilometer (Form Talysurf 120, Taylor Hobson, Leicester, UK).

2.7.3.2. Scanning electron microscopy (SEM). The surface morphology of the worn samples was observed by SEM. A ZEISS EVO 50 XVB apparatus (Oberkochen, Germany), equipped with LaB_6 source, was used. To avoid the charge effect, all the samples were metalized before the analysis with a 5 nm layer of gold.

Table 1
Inputs and outputs on the synthesis process referred to 1 functional unit of 1 kg of epoxy resin.

Material for recipe	Material from ecoinvent database	Amount
MATERIALS AND ENERGY INPUTS		
Base resin	Liquid epoxy resin	0.667 kg
Fat acids	Stearic acid	0.333· 0.465 *B_fraction* kg
Benzyl alcohol	Benzyl alcohol	0.333·0.365 *B_fraction* kg
Meta-phenylenediamine	Meta-phenylenediamine	0.333·0.11 *B_fraction* kg
4-4′-isopropilidendiphenol	Bisphenol A, powder	0.333·0.04 *B_fraction* kg
N,N-dimethyl-1,3-diaminopropane	dimethylaminopropylamine	0.333·0.02 *B_fraction* kg
Bio-oil	–	0.333·(1-*B_fraction*) kg
Electricity	Electricity, low voltage, IT	4.774 MJ
MATERIAL OUTPUT		
Epoxy resin	–	1 kg

2.8. Life cycle assessment (LCA)

2.8.1. General method

The method standardized by ISO 14044 was adopted, and, for this work, the open-source software OpenLCA v2.1.0, the ecoinvent database v3.8, and primary data from Assocanapa s. r.l. were used.

2.8.2. Application of the LCA method to the bio-oil-based resins and the commercial recipe

For the sake of this assessment, a functional unit (FU) of 1 kg of epoxy resin was considered. A comparative LCA was carried out where the four different bio-resins and the commercial epoxy resin were investigated. The commercial epoxy resin was modeled assuming a content of bio-oil equal to zero; this way, the same model for the production chain was considered for all variants.

In any LCA study, to obtain reliable results, it is of paramount importance to set proper system boundaries that identify the processes included in the assessment and those that are excluded accompanied by

Table 2
Values of the parameter *B fraction* to be assumed for modelling the different epoxy resin recipes.

	Base resin (Component A)	Curing agent (Component B)		*B fraction*
		Bio-oil	Amine	
EP commercial	2/3		1/3	1
EP bio 1:8	2/3	1/27	8/27	0.888888
EP bio 1:4	2/3	1/15	4/15	0.8
EP bio 1:2	2/3	1/9	2/9	0.666666
EP bio 1:1	2/3	1/6	1/6	0.5

a full explanation of the reasons for the exclusion. It is just worth recalling here that excluding processes from a product system may change the final impact results considerably, thus affecting the overall representativeness of the assessment outcomes.

Fig. 1 illustrates the schematic representation of the system boundaries considered for the bio-resin LCA. Green boxes represent flows for which background production processes are available in the ecoinvent database.

The synthesis process, which receives the contribution of bio-oil (or not, in the case of the commercial epoxy resin) was modeled as indicated in Table 1.

In Table 1, the amount of each ingredient of the B component (representing 1/3 of the total mass) was calculated according to the concentration reported in the safety data sheet of a typical commercial product, i.e., a B component that contains 46.5% of fatty acids, 36.5% of benzyl alcohol and other minor components.

The *B fraction* parameter was assumed as defined in Table 2 to model the various recipes of resin. Also, it should be noted that the synthesis process was considered as performed in Italy adopting the related electricity mix.

The impact assessment was performed by adopting the Environmental Footprint 3.0 method and the Cumulative Energy Demand method.

3. Results and discussion

3.1. Bio-oil characterization

Table 3 summarizes the concentrations of 50 bio-oil components that were determined by GC/MS. The total % concentration of the components reported in Table 3 corresponds to 63% of the analyzed material. According to the results, it can be said that pyrolytic oil is mainly composed of: 1) furan compounds, derived from the degradation of cellulose chains and the short non-aromatic chains of the lignin structure (Hassan et al., 2009); 2) aromatic compounds, obtained from the primary degradation of the aromatic structures of the lignin itself; 3) long-chain fatty acids, realistically extracted in a steam current during the first stages of pyrolysis, which do not undergo decarboxylative degradation (the loss of carbonyl); 4) acetic acid, formed through advanced decomposition reactions mainly in the vapor phase (Bartoli et al., 2020); 5) nitrogenous compounds, as pyridine, related to the degradation of the residual protein material, through radical cyclization reactions and inclusion in aromatic products (Zong et al., 2020). The bio-oil itself contains furan and phenolic species that can be harmful, and they generally represent a weak point for pyrolytic conversion due to the difficulties of their use under safe conditions. Our approach allows for the entrapment of these species into the epoxy network, hence preventing their release, also thanks to their participation in the curing process.

3.2. Structural and thermal characterization of bio-resins

This section aims to analyze the chemical changes of the resin system due to the partial replacement of the amine-based hardener by the bio-oil. In particular, DSC and FTIR analyses allowed us to verify the full

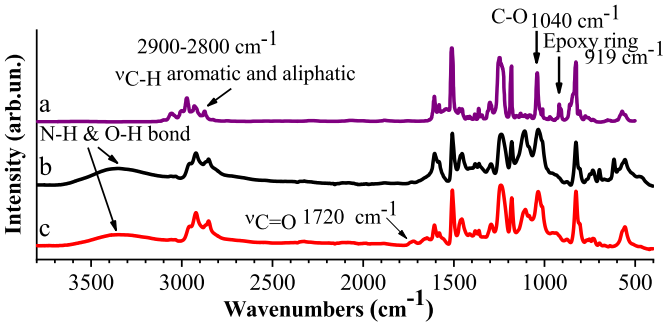

Fig. 2. ATR spectra of diglycidyl ether of bisphenol A (DGEBA), before (a) and after (b) curing and of EP bio 1:1 cured resin (c).

Table 3
GC-MS characterization of pyrolysis bio-oils obtained from hemp hurd.[a]

Compound name	C (%)	Rt (min)	CL (%)	Compound name	C (%)	Rt (min)	CL (%)
4-methyl-2-undecene	0.6	6.11	46	4-ethyl-2-methoxyphenol	0.9	49.67	76
2- methyl-3-eptene	0.4	6.19	46	Cyclobutanol	0.5	51.88	53
Pyridine	0.3	7.95	91	p-cresol	1.2	52.48	95
3- methyl -1-butanol	0.6	8.79	90	3-ethylphenol	0.7	52.83	96
1-hydroxypropan-2-one	0.8	12.38	80	Caprolactam	1.4	55.85	95
4-Isopropyl-1,3-cyclohexanedione	1.4	14.11	60	4-ethylphenol	1.0	56.63	91
3,4-dimethyl -3- cyclopenten-1-one	0.5	18.77	49	2-methoxy-4-vinylphenol	0.5	57.21	95
Acetic acid	1.8	20.29	91	Methyl hexadecanoate	0.7	58.26	92
2-propanone	0.3	20.81	46	2,6-dimethoxy-phenol	1.5	59.96	96
1-(2-furanyl)-ethanone	0.4	22.53	70	Fluorene	0.4	61.35	93
3- methyl -2- cyclopenten -1-one	0.4	22.67	94	Isoeugenol	0.7	62.77	97
1,2,4-trimethyl-cyclohexane	0.6	23.7	49	3,5- dimethoxy-4- hydroxytoluene	0.5	62.98	93
Gamma-Butyrolactone	0.3	28.74	80	1,4:3,6-Dianhydro-α-d-glucopyranose	0.3	64.31	94
p-Mentha-1,8-dien-4-ol	0.4	29.65	43	Ethylsuccinate	4.2	64.45	83
Acetophenone	0.7	29.96	91	2,3,5-Trimethoxytoluene	1.3	64.90	90
2-Furanmethanol	0.8	31.37	94	Benzoic acid	5.6	65.82	95
2-hydroxy-3- methyl-2-Cyclopenten-1-one	0.8	39.73	96	4-methylbenzoic acid	0.6	69.00	97
1,2,4- trimethyl -4-Isopropylcyclohexane	0.6	40.07	50	1,2,3,5-tetramethylcicloexane	0.5	70.48	47
2-methoxyphenol	0.8	41.36	95	Ethylbenzoic acid	0.5	71.64	96
Creosol	0.3	46.10	95	Tetradecanoic acid	0.8	73.45	98
Biphenyl	0.6	46.94	95	(E)-2,6- dimethoxy-4-(prop-1-en-1-il)phenol	0.7	74.08	94
2-Phenylethanol	2.0	48.88	94	Pentanoic acid	0.5	76.14	99

[a] C is the % concentration calculated from the peaks area, Rt is the retention tine and CL is the confidence level of the molecular identification.

Table 4
Gel fraction (%) and cross-link density evaluated for the bio-resin by swelling test using methanol as solvent. The Flory-Huggins interaction parameters (χ) between epoxy network and methanol is equal to 1.103.

	Gel fraction (wt.%)[a]	Crosslinking density (mol/cm^3 10^4)
EP	80.2	50.6
EP bio 1:8	78.9	32.0
EP bio 1:4	75.9	13.2
EP bio 1:2	74.2	2.56
EP bio 1:1	55.9	n.d.[b]

[a] The samples undergo leaching during swelling tests losing more than 20 wt %.
[b] n. d. = non-determinable.

degree of curing. The crosslinking density was measured through swelling experiments. WAXS and SAXS analyses allowed us to confirm the formation of a network due to the reaction of DGEBA epoxy groups with residual amine-based hardener and the possible occurrence of phase separation as a function of the bio-oil content.

Fig. 2 reports the typical FT-IR spectra in ATR mode for DGEBA, commercial EP, and EP bio 1:1. A detailed description of the main bands is reported in Fig. S3. Here, the spectra are used to confirm the completeness of the curing process for EP and bio-resins. C-H stretching of the terminal oxirane group is observed at 3050 cm^{-1}, whereas ν_{CH} of CH_2 and CH aromatic and aliphatic groups occurs in the range 2990–2880 cm^{-1}. Ethers $\nu_{C\text{-}O\text{-}C}$ stretching appears at around 1040 cm^{-1} and oxirane $\nu_{C\text{-}O}$ at around 919 cm^{-1}. The latter is commonly used in quantitative studies of epoxy curing (Celikbag et al., 2017). Both commercial resin and bio-resins present similar spectra. The signals of the oxirane $\nu_{C\text{-}O}$ in all the resins are not evident: this finding indicates that all the epoxy rings of DGEBA successfully reacted with the hardener even when 50% of amine hardener (i.e., EP bio 1:1 sample) is replaced with the bio-oil. Besides, the ν_{NH} and ν_{OH} stretching vibrations appear as a broad band in the region of 3200–3600 cm^{-1}: they are typically attributed to the presence of curing agent and hydroxyl groups that are formed during the curing process. The only difference among cured resin spectra refers to the intense bands, present only in the spectrum of the bio-resin at around 1770 cm^{-1}, which are attributable to carbonyl, carboxyl, and ester bonds present in the bio-oil. These bands are not visible in the commercial epoxy resin.

DSC measurements, presented in Fig. S4, confirm that the curing was complete for all the resins. In fact, the thermograms do not show any exothermic peak above the glass transition, excluding the occurrence of post-curing processes.

The values of crosslinking density (Table 4) tend to decrease as the bio-oil content increases, suggesting the reduced participation of bio-oil components in the network formation. As a matter of fact, the cured bio-oil-containing resins experience a non-negligible weight loss even in the absence of bio-oil during the swelling tests performed in methanol. As the bio-oil content increases, the weight loss increases, approaching about 50 wt% for the sample EP bio 1:1, for which swelling was negligible.

The WAXS profiles of EP resins (Fig. 3A) show two humps at $2\theta \approx 4$ and 18°, corresponding to correlation distances of 2 and 0.5 nm, respectively; their position and the relative intensities are similar, regardless of the bio-oil content. These diffraction profiles indicate that the samples are amorphous. In particular, the two humps are due to the reaction of amine and oil components with DGEBA; the main peak at $2\theta \approx 18°$ is ascribable to intramolecular correlations, whereas the peak at $2\theta \approx 4°$ can be attributed to the average distance between the amine groups and/or oil components pendant from DGEBA (Kumar and Adams, 1987; Lovell and Windle, 1990). The relative intensity of the diffraction peak at $2\theta \approx 4°$ depends on the crosslinking density achieved during the curing process for amine-cured EPs (Lovell and Windle, 1990). Therefore, the finding that the relative intensity of two diffraction peaks at $2\theta \approx 4$ and 18° is not significantly changed by replacing part of amine linkers with bio-oil (Fig. 3A) suggests that the epoxy groups of DGEBA react partly with amine groups forming active crosslinks, and partly with some components of bio-oil, even though the resulting moieties do not necessarily participate in the network formation. The presence of pendant groups from DGEBA units confirms that the network structure of cured EP resins is strongly modified by the presence of the bio-oil. As a matter of fact, EP bio 1:1 sample does not form an efficient network: this statement is supported by the corresponding WAXS profile, which is similar to that of the neat EP resin in the absence of bio-oil.

The systems containing bio-oil/amine ratios of 1:8 (EP bio 1:8) and 1:2 (EP bio 1:2) show flat SAXS profiles (Fig. 3B), which are similar to each other. A similar SAXS profile is shown by EP bio 1:4 sample. The SAXS profiles are featureless, indicating the absence of heterogeneities at length scales (correlation distances) comprised in between 4.5 ($\approx 2\pi/q_{max}$, q_{max} = 0.12 nm^{-1}) and 52 nm ($\approx 2\pi/q_{min}$, q_{min} = 1.4 nm^{-1}). Conversely, the SAXS profiles of the system containing the highest bio-oil quantity (EP bio 1:1) show an upturn at low q values (Fig. 3B), probably because of the occurrence of phase separation in domains rich and domains poor in bio-oil, separated by smooth interfaces, as evidenced by the fact that the SAXS profile at $q > 0.27$ nm^{-1} follows the Porod law.

The values of the storage and loss moduli curves are reported in Fig. 4A and C, respectively. In general, by increasing the amount of bio-

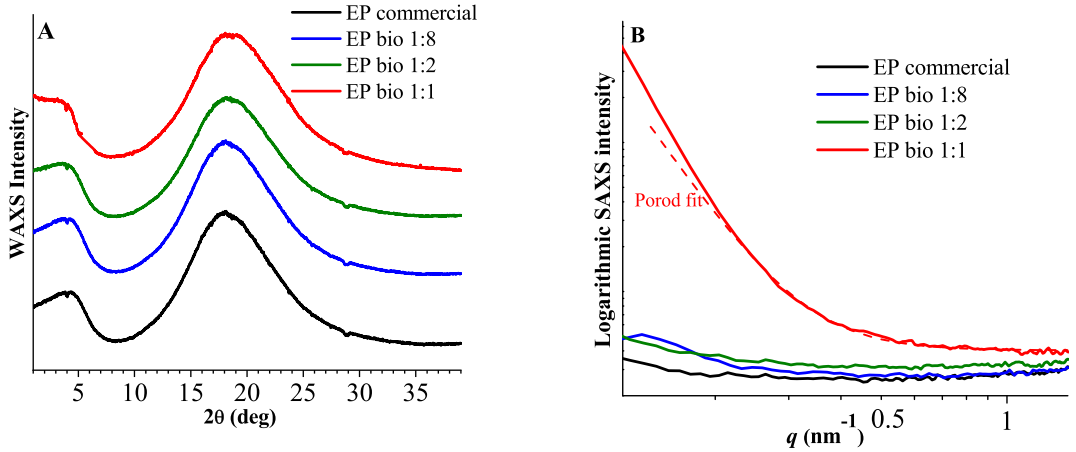

Fig. 3. Wide angle X-ray powder diffraction (WAXS) and small angle X-ray diffusion profiles of EP resins cured with and without (EP commercial) adding the bio-oil, using bio-oil/amines ratio 1:8 (EP bio 1:8), 1:2 (EP bio 1:2) and 1:1 (EP bio 1:1). Similar WAXS and SAXS profiles are shown by EP bio 1:4 sample. The dashed line in B is the fit to the data for $q > 0.27$ nm^{-1} with the Porod law overlaying a flat background I_{bak}, that is $I_{bak} + K_p\, q^{-4}$ (Glinka, 2001).

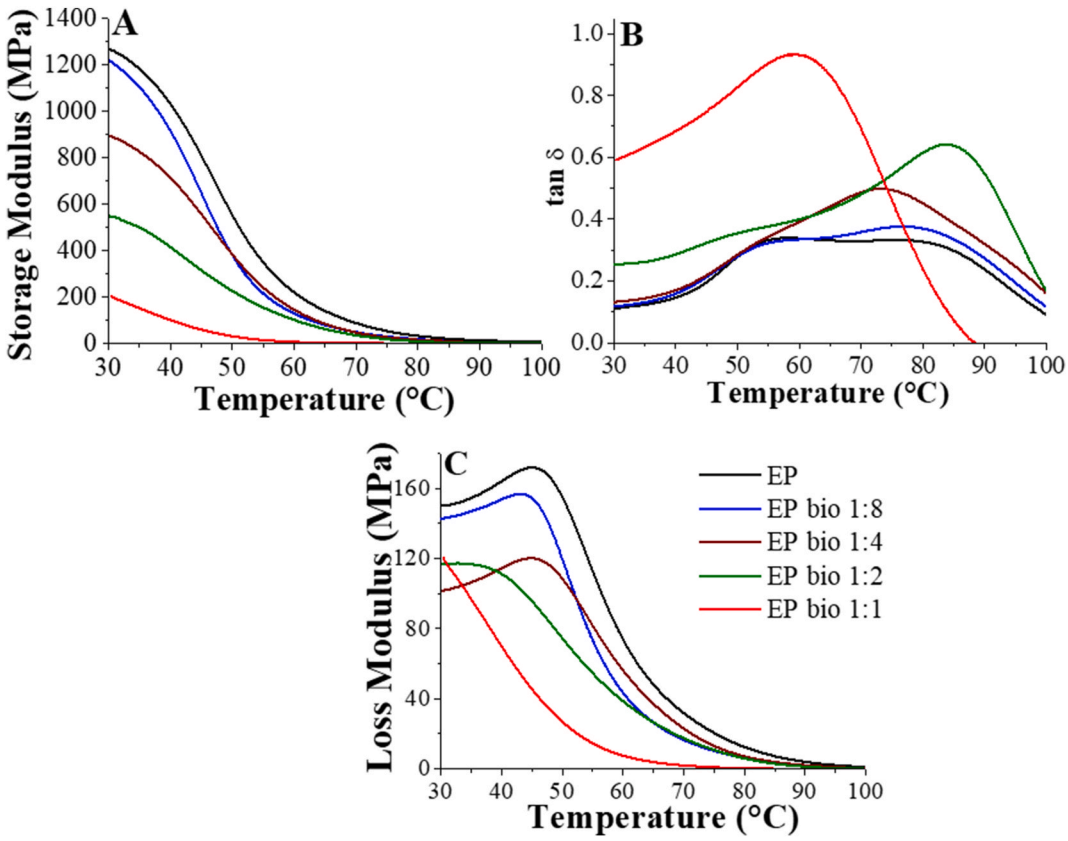

Fig. 4. A) Storage modulus, B) tan δ and C) loss modulus curves of EP resins.

oil, the values of storage and loss moduli in the glassy state decrease. As an example, at 30 °C, commercial EP and EP bio 1:8 show a storage modulus of 1264 MPa and 1212 MPa, respectively (the loss modulus is 150 and 143 MPa, respectively), which decrease to 891, 548, and 204 MPa for EP bio 1:4, EP bio 1:2 and EP bio 1:1, respectively (the loss modulus is 117, 101 and 120 MPa, respectively). Increasing the bio-oil content promotes a reduction of active crosslinks among DGEBA units, leading to a more flexible and less rigid structure, which accounts for a decay of the storage modulus (Rahul and Kitey, 2016). Fig. 4B compares the tan δ curves for all the investigated systems. EP and EP bio-resins 1:8, 1:4 and 1:2 present two sub-glass relaxation peaks: the former, located at lower temperature, corresponds to the local crankshaft motions of hydroxypropyl ether segments $-CH_2-CH(OH)-CH_2-$ of the network and to aromatic ring flips of DGEBA (García et al., 2000; Heux et al., 1997), while the latter relaxation is due to the motion of molecular segments of greater length or lesser mobility than those responsible for the T_g.

As tan δ represents the ratio between the dissipative and storage modulus, its value provides information on the material's ability to dissipate the mechanical energy when subjected to cyclic loading or deformation. In simpler terms, it represents how well a material absorbs and dissipates energy when it undergoes mechanical stress, such as bending, stretching, or vibration. Hence, tan δ values quantify the damping capacity of a material. The bio-resin systems show higher damping capacity than commercial EP due to the greater mobility of the molecular chains because of the presence of bio-oil. The tan δ observed for the EP bio 1:1 sample has a very different shape: tan δ curve is characterized by a single peak much more intense than those recorded for other bio-resins.

Based on these results, the bio-oil, being a mixture of different components, partly acts as a curing agent and partly as a filler. This is demonstrated in the next section, by measuring Martens hardness, indentation Young's modulus, and wear behavior.

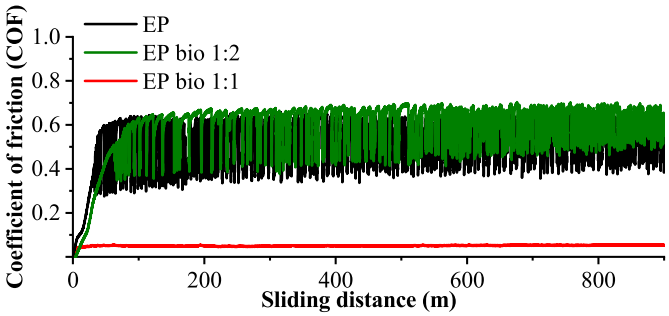

Fig. 5. Friction coefficient (COF) as a function of the sliding distance (m) for the EP blank and the EP-bio-resins.

3.3. Mechanical behavior of bio-resins

Table 5 collects the Martens Hardness (H_m) and the indentation Young's modulus (E_{IT}) observed for each resin. EP shows a H_m of 174.2 ± 6.8 N/mm^2. The partial replacement of the hardener with the bio-oil leads to a decrease in the hardness of the material up to a minimum value of 139 ± 13 N/mm^2 reached for the EP bio 1:2 system. Similarly, E_{IT} goes from 3.4 ± 0.1 GPa (for commercial EP) to 2.2 ± 0.2 GPa (for EP bio 1:2). Under the same experimental conditions, the elastic response to the stress of the microindenter for EP bio 1:1 sample is undetectable. The bio-resins become softer as the quantity of bio-oil added to the formulation increases. This effect is due to the decrease in the crosslinking density, leading to a more flexible and less rigid structure.

Fig. 5 shows the COF as a function of the sliding distance for the commercial EP, EP bio 1:2, and EP bio 1:1. For clarity, the COF values of EP bio 1:8 and EP bio 1:4 samples are reported in Fig. S5. Table 4 provides a summary of the average COF and the related wear parameters

Table 5
Hardness (N/mm^2), Indentation Young modulus (E_{IT}), average friction coefficient (COF), wear depth and wear rate of EP and bio-resins.

	Hardness (H_m) (N/mm^2)	Indentation Young Modulus (E_{IT}) (GPa)	COF	Track Depth (μm)	Specific Wear rate k (x 10^{-4} mm^3/N·m)
EP	174 ± 7	3.5 ± 0.1	0.62 ± 0.02	86 ± 15	3.62
EP bio1:8	145 ± 3	2.7 ± 0.1	0.64 ± 0.01	53 ± 11	2.06
EP bio 1:4	140 ± 7	2.3 ± 0.1	0.56 ± 0.03	47 ± 10	1.66
EP bio1:2	139 ± 13	2.2 ± 0.2	0.62 ± 0.01	35 ± 8	0.40
EP bio1:1	n.d.[a]	n.d.[a]	0.050 ± 0.004	n.d.[a]	n.d.[a]

n.d. = not determinable.

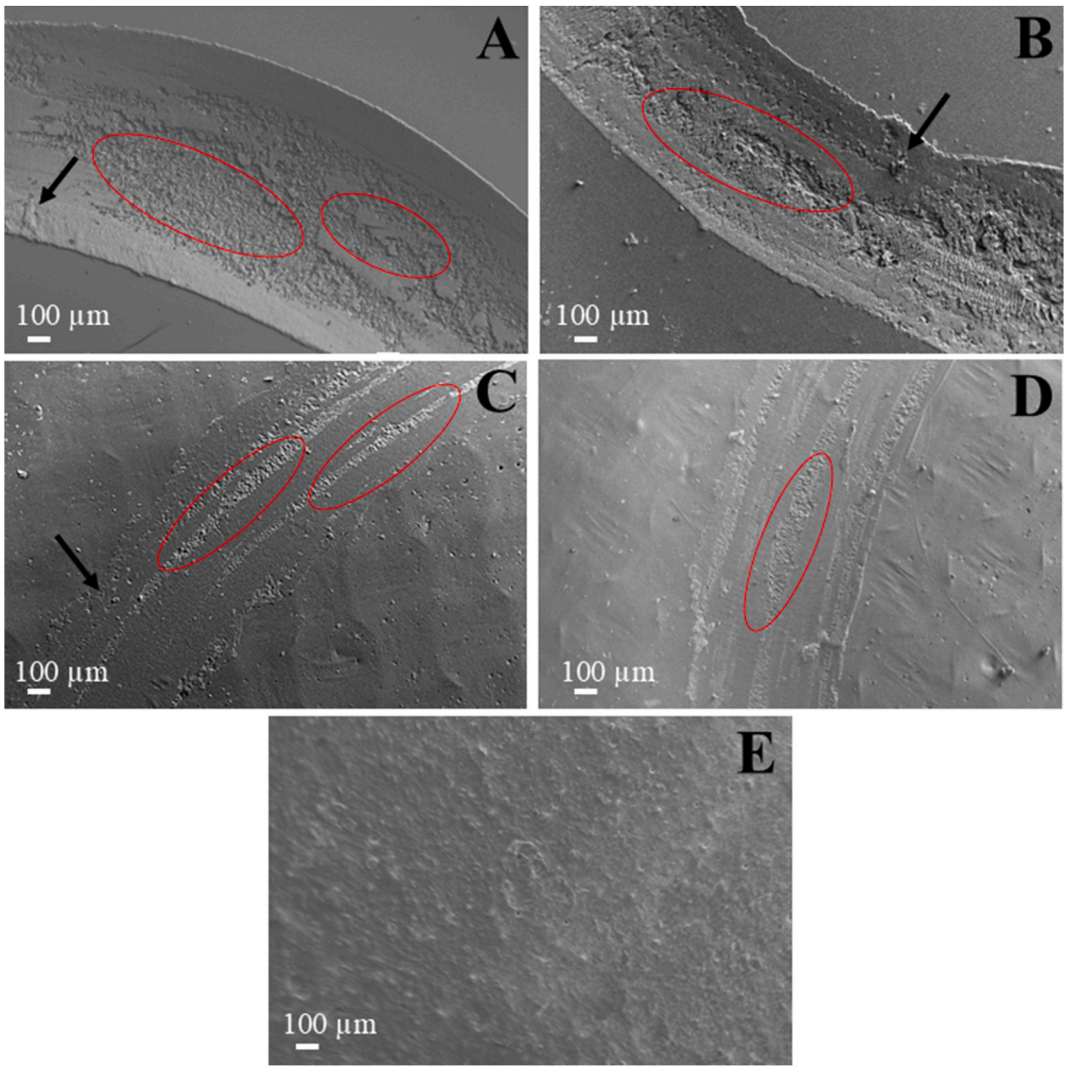

Fig. 6. SEM micrographs of worn surfaces of the epoxy systems: A) EP, B) EP bio 1:8, C) EP bio 1:4, D) EP bio 1:2, and E) EP bio 1:1. The red circles in A-D delimit the areas that underwent severe wear losses. Debris attributable to adhesive-type wear mechanisms are highlighted with the black arrow. In EP bio 1:1 (E), no wear tracks are observed: heterogeneity is due to phase separation. (For interpretation of the references to colour in this figure legend, the reader is referred to the Web version of this article.)

(wear depth and specific wear rate). The stick-slip phenomenon is observed for all the investigated resins but EP bio 1:1. This phenomenon refers to intermittent motion observed when two surfaces in contact experience both static (stick) and kinetic (slip) friction and provides COF curves with a peculiar oscillating trend due to harder steel ball's plowing motion on the softer substrate (Menezes et al., 2009; Jiang et al., 2015).

EP shows a COF of 0.62 (Table 5), which is in agreement with the value obtained for a similar resin investigated in a previous work (Bartoli et al., 2022). The COF recorded for EP bio 1:8, EP bio 1:4, and EP bio 1:2 is not substantially different from that of EP. This result agrees with the literature, which indicates that DGEBA plays the main role in the friction behavior (Correa et al., 2015). In stark contrast to other materials in the study, the EP bio 1:1 system exhibits a COF as low as 0.05, which is an order of magnitude lower than that observed for standard EP resins and other bio-resins. This remarkable reduction in friction can be attributed to the unique viscoelastic properties inherent in EP bio 1:1. These properties are a direct consequence of its distinct structural composition, as revealed by SAXS analysis: the structure of EP bio 1:1 is characterized by domains of different compositions, where those rich in bio-oil act as natural lubricants, significantly reducing frictional forces during contact (Zhang et al., 2024a, 2024b).

For the commercial resin, the wear track shows an average depth of

Table 6
Impacts due to the production of 1 kg of epoxy resin with the recipe EP bio 1:1 and commercial (no bio-oil). The last column collects the changes of each impact passing from the commercial system to the bio-based counterpart.

Impact categories	Unit	EP bio 1:1	EP	Reduction
Acidification	mol H+ eq	0.02327	0.02369	2%
Climate change	kg CO_2 eq	5.0816	5.23311	3%
Ecotoxicity, freshwater	CTUe	233.737	262.77585	11%
Eutrophication, freshwater	kg P eq	0.00142	0.00136	−4%
Eutrophication, marine	kg N eq	0.02127	0.03771	44%
Eutrophication, terrestrial	mol N eq	0.04463	0.04538	2%
Human toxicity, cancer	CTUh	$5.01{\cdot}10^{-9}$	$5.25{\cdot}10^{-9}$	5%
Human toxicity, non-cancer	CTUh	$7.36{\cdot}10^{-8}$	$9.25{\cdot}10^{-8}$	20%
Ionizing radiation	kBq U-235 eq	0.42778	0.38917	−10%
Land use	Pt	21.52384	9.98998	−115%
Ozone depletion	kg CFC11 eq	6.87E-07	$6.80{\cdot}10^{-7}$	−1%
Particulate matter	disease inc.	$1.86{\cdot}10^{-7}$	$1.92{\cdot}10^{-7}$	3%
Photochemical ozone formation	kg NMVOC eq	$1.59{\cdot}10^{-2}$	$1.64{\cdot}10^{-2}$	3%
Resource use, fossils	MJ	89.97609	93.92578	4%
Resource use, minerals and metals	kg Sb eq	$5.50{\cdot}10^{-5}$	$5.57{\cdot}10^{-5}$	1%
Water use	m^3 depriv.	3.51262	3.01984	−16%

Legend: CTUh = Comparative Toxic Unit for human; CTUe = Comparative Toxic Units for ecotoxicity; disease inc. = disease incidences (Human health effects associated with exposure to PM2.5); m^3 depriv = User deprivation potential (deprivation-weighted water consumption); kBq = kilobecquerel; U-235 eq = Uranium-235 equivalent; NMVOC = Non-Methane Volatile Organic Compounds; CFC11 = trichlorofluoromethane; Sb = antimony; N = nitrogen.

86 ± 15 μm and a specific wear rate of 3.62×10^{-4} $mm^3/N{\cdot}m$. These values decrease as the quantity of employed bio-oil increases in the epoxy formulation. In particular, EP bio 1:2 sample exhibits a decrease in the average depth and the specific wear rate of 59 and 89%, respectively. As for the hardness, the tribological tests performed on EP bio 1:1 do not produce any wear trace detectable by the profilometer (also confirmed by SEM observation), suggesting that in the experimental conditions used in this work, the surface, if worn, is so below the instrumental sensitivity. The results can be interpreted considering what has been discussed so far: the lubricant effect of the bio-oil, combined with the significant increase in damping ability (evidenced by DMTA analysis) increases the wear resistance. This finding is in agreement with the decrease in H_m and E_{IT}, which also become progressively lower as the amount of bio-oil in the materials increases. The values of average depth, the specific wear rate, H_m, and E_{IT}, indeed, are strictly dependent on the crosslinking density. In fact, as shown in Table 4, the crosslinking density decreases with increasing the bio-oil content. The overall effect is to improve the durability of epoxy resins, providing them with sustainable properties.

To support these considerations, the worn surfaces were observed by SEM. Fig. 6 shows the micrographs of all the epoxy systems investigated. The wear track of commercial EP is clearly deeper and wider than that observed for the bio-resins, confirming the previously discussed results. Moreover, EP shows severe wear losses characterized by adhesion signs. In some areas of the track, it is possible to observe the presence of debris as indicated by the black arrow. Wear is increasingly reduced by increasing bio-oil content. The worn track of EP bio 1:2 (Fig. 6D) is smoother with reduced signs of adhesions (in number and dimension). For EP bio 1:1 (Fig. 6E), no wear tracks are observed, but only heterogeneity due to phase separation, as confirmed by SAXS analysis.

Also, the surface of the steel ball against EP bio-resins (Fig. S6 from B to E) appears smoother and less worn than that of the steel ball against commercial EP (Fig. S6A) due to the increase in softness of the materials as the amount of bio-oil increases. This is indicated by the presence of stripes in the SEM micrographs of the steel ball against neat EP resin, evidenced by arrows (Fig.S6A). Also, the steel ball against EP bio 1:8 and EP bio 1:4 shows a region with a severe loss (arrows in Figs. S6B and S6C).

In conclusion, the replacement of amine curing agents with bio-oil induces a decrease in Martens hardness and indentation Young's modulus and specific wear rate, while COF values remain constant

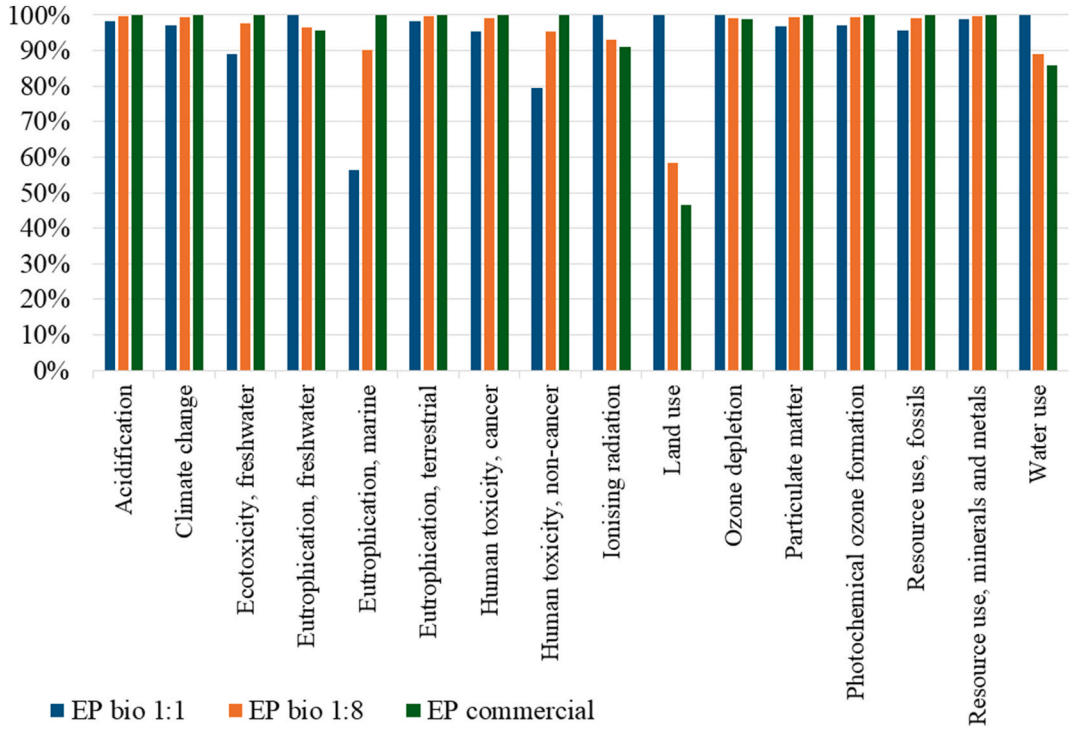

Fig. 7. Comparison of all impacts due to the production of 1 kg of epoxy resin according to the different formulations considered in this work. EF 3.0 method is applied.

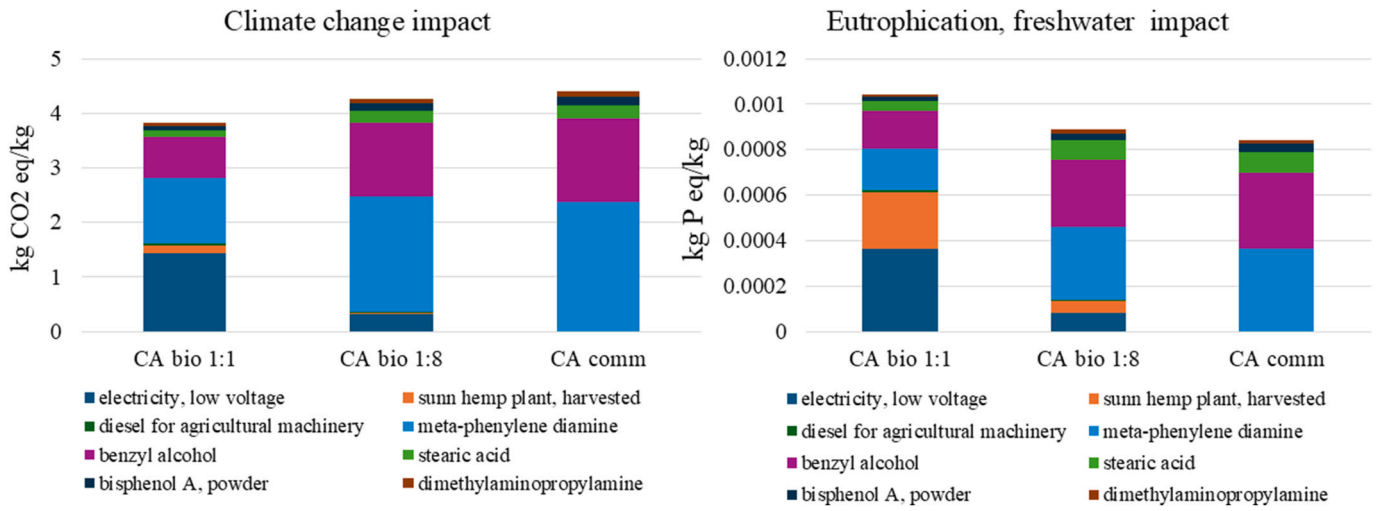

Fig. 8. Role of the hemp cultivation and of the substitution of traditional curing agent ingredients in two major impacts. CA = curing agent.

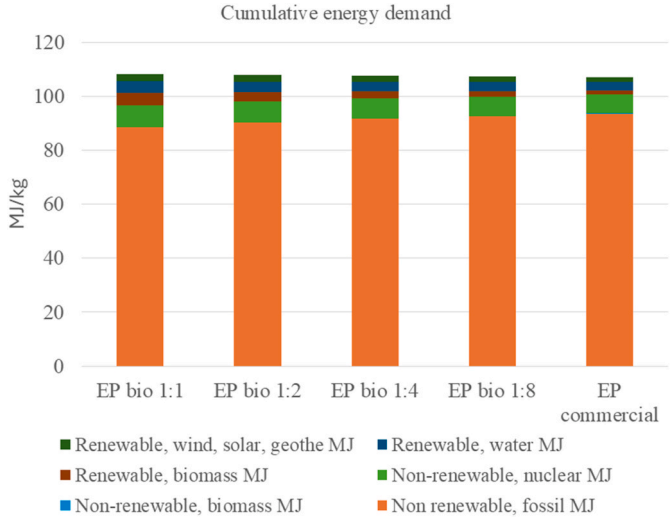

Fig. 9. Cumulative Energy Demand impact calculated for the production of 1 kg of epoxy resin.

except for EP bio 1:1. This means that bio-oil increases the intrinsic flexibility of the resultant bio-resin, partly due to the lubricant effect exerted by the bio-oil, partly to the decrease in the crosslinking density, thus widening the range of properties that EP resins approach. The use of the bio-resins formulated here represents a remarkable green aspect in the field of construction and lamination in the building sector.

3.4. LCA results

OpenLCA allows for obtaining life cycle impact assessment results in many varied forms. Fig. S7 shows a Sankey diagram representing the contribution to the Climate Change impact of the production of EP bio 1:1 system, where it is possible to appreciate the influence of the DGBMA to the specific impact. Partially replacing the amine-based curing agent, in this formulation, with bio-oil, accounts for a reduction in climate change, marine eutrophication, human toxicity (non-carcinogenicity), and ecotoxicity by around 3, 44, 20, and 11%, respectively. These attenuations can be seen quantitatively both in Table 6, where EP bio 1:1 and EP are compared, and in Fig. 7 where, by normalizing at the highest value, it is possible to appreciate the variation of each impact for commercial EP, EP bio 1:8 and EP bio 1:1.

The increase in land use, eutrophication of freshwater, and water use are clearly due to the cultivation and agricultural practices of hemp, while the increase in ionizing radiation is ascribed to the need for more electricity during the pyrolysis process, which is not necessary for the production of EP. All other impacts decrease, although often not significantly.

After having identified DGBMA as the most impacting ingredient of the epoxy resin, one further assessment was made, reducing the boundaries of the analysis to focus on the curing agent only. Graphs in Fig. 8 show the respective contributions to climate change and eutrophication of freshwater due to the production of the curing agent for EP bio 1:1, 1:8, and for EP. The electricity needed for the synthesis has been neglected for the three solutions as it is the same for all.

Finally, energy consumption was additionally evaluated through the Cumulative Energy Demand method. Fig. 9 shows the result of this assessment: it is worth noticing that the energy consumption required for preparing the bio-based resins increases. As said, an additional pyrolysis process is needed for these solutions, but also a contribution in terms of biomass is considered during the cultivation steps as modeled in ecoinvent. However, considering the role of the DGEBA resin in climate change impacts, it can be concluded that also the energy consumption baseload is due to this production process, which in this study was taken as an average European process, supplied according to an average European electricity mix.

The LCA results may appear only slightly favorable for the bio-based epoxy systems. However, it should be noted that this assessment does not include the use phase in the system boundaries. As demonstrated in § 3.3, some combinations of bio-oil and traditional curing agent ingredients, such as in the case of EP bio 1:2, show a wear rate that is much lower than that of the commercial product. This leads to a longer technical life of the bio-based products, leading to two possible interpretations: less bio-based material is needed to satisfy the use requirements, or a much longer life is guaranteed by the bio-based material, resulting in a much lower substitution rate during the use phase. Whatever the interpretation, the LCA can include the use phase assuming a different functional unit that takes into account the specific wear rate, a sort of "equivalent mass" of EP resin calculated as:

$$m_{EP\ bio} = m_{commercial} \cdot \frac{k_{w,EP\ bio}}{k_{w,commercial}} \quad (5)$$

where the coefficients to be applied to the assessment are listed in Table 7.

No value is considered for EP Bio 1:1 as no detectable wear was observed. Considering these equivalents, the new assessment with FU 1 kg of mass equivalent of EP resin provides the results shown in Fig. 10.

Table 7
Equivalent mass coefficient for the different resins.

EP resin	Equivalent mass coefficient $m_{EP\ bio}$
EP commercial	1
EP bio 1:8	0.569
EP bio 1:4	0.459
EP bio 1:2	0.110

The increased resistance can impact very positively in the results of LCA allowing for a reduction of all impacts when the use phase is considered.

LCA results for the production and use of all variants of bio-based resin are promising as they show a reduction in all impacts, including energy consumption, carbon footprint, and consumption of resources. This performance is increasingly relevant considering the current and future requirements dictated by the new European ecodesign directive (ESPR – ecodesign requirements for sustainable products) (Regulation (EU) 2024/1781, 2024). In particular, the performance in terms of wear resistance of the new material complies with the requirement of product durability, which is one of the cornerstones of the regulation. The regulation belongs to the wider framework of the Green Deal programme and walks alongside the Green Claim Directive: the LCA results are the favorite supporting data and pieces of evidence for promoting the materials, products, and services on the market according to the scheme put in place by the Commission to combat greenwashing. The industrial exploitation of the positive LCA results of bio-based resins can be achieved, for example, through the implementation of the EPD (Environmental Product Declaration) scheme for better and scientifically sound communication to stakeholders about the environmental quality of the product. This plus normally coincides with an economic advantage for producers/suppliers of materials, products, and services.

4. Conclusions

This study demonstrated that bio-oil derived from the pyrolysis of hemp hurd side stream can be used as a partial replacement for the amine curing agent in the production of commercial epoxy systems. The reduction in active crosslink density due to the presence of bio-oil resulted in a more flexible structure, which caused a decrease in Martens hardness and indentation modulus, but improved damping and wear resistance as the amount of bio-oil added to the formulation increased. Compared to the commercial resin, the average wear track depth and specific wear rate decreased by 59 and 89%, respectively, when 50% of the amine-based hardener was replaced with the bio-oil. Interestingly, the bio-resin containing equal amounts of bio-oil and amine hardener exhibits a completely different viscoelastic behavior, which is influenced by bio-resin structure, as revealed by SAXS analysis, which consists of domains of different compositions, with the bio-oil-rich domains acting as lubricants. For this sample, no wear trace was detectable, suggesting that in the adopted experimental conditions, wear phenomena were below instrumental sensitivity. The Life Cycle Assessment, which also included the extraction of hemp hurd using a prototype for mechanical separation of fibers and hurd from hemp bales, showed only a slight advantage for the bio-based solutions. Compared to the production of the commercial resin, the production process of the bio-resins showed marginal advantages for 11 out of 16 impact categories. However, when the technical life (i.e., wear resistance) of the bio-based products was considered, a significant reduction in all impacts was observed. When the bio-oil was half that of the amine-based hardener, all impacts were reduced by more than 80%.

In conclusion, the present manuscript provides the basis for replacing amine curing agents with bio-oil, a component derived from renewable resources, to obtain epoxy systems with improved properties and reduced environmental impact. The use of the here-formulated bio-resins represents a remarkable green aspect in the field of construction

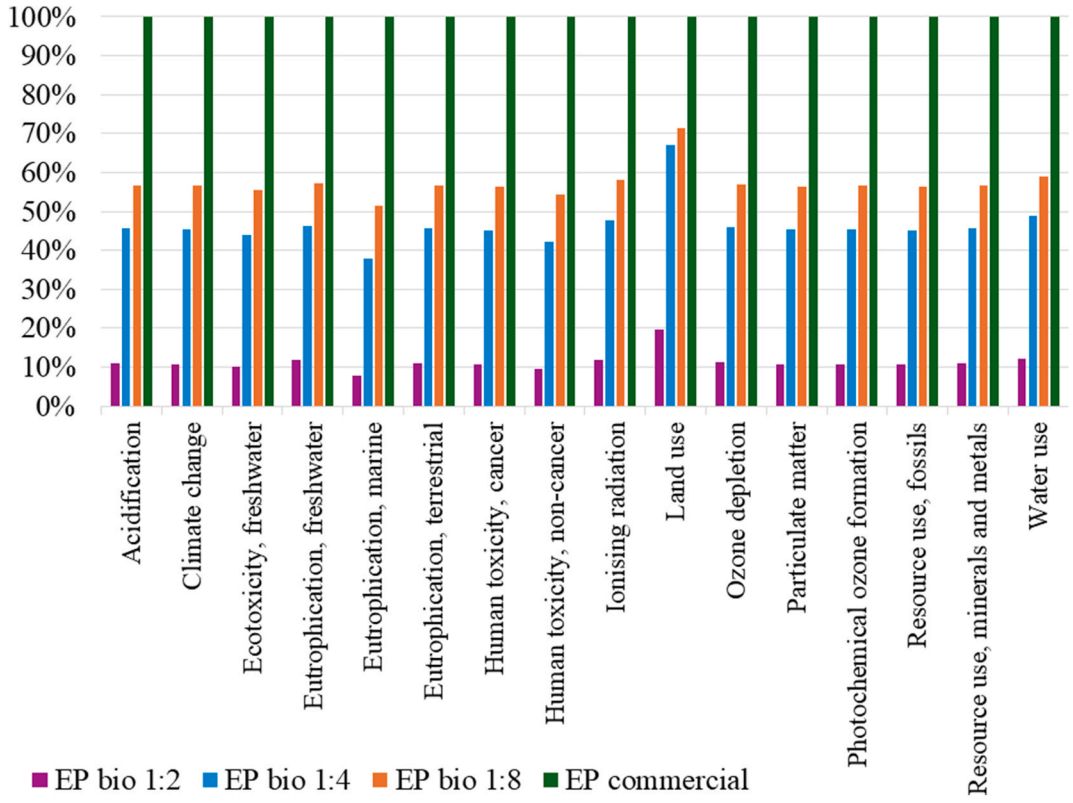

Fig. 10. Comparison of all impacts due to the production of 1 kg equivalent of epoxy resin according to the different formulations considering the use phase. EF 3.0 method applied.

and lamination in the building sector. Future work can be envisaged to extend the study to such other biomasses as food and forest wastes. Furthermore, having identified DGBMA as the most impactful component of the epoxy systems through LCA analysis, the replacement of this harmful petroleum-based monomer needs to be addressed and implemented.

CRediT authorship contribution statement

D. Duraccio: Writing – review & editing, Writing – original draft, Supervision, Methodology, Formal analysis, Conceptualization. **M. Di Maro:** Writing – review & editing, Writing – original draft, Formal analysis. **F. Vaccaro:** Formal analysis. **M.G. Faga:** Writing – original draft, Conceptualization. **M. Bartoli:** Supervision, Formal analysis, Conceptualization. **G. Malucelli:** Writing – review & editing, Writing – original draft, Resources, Conceptualization. **F. Auriemma:** Writing – original draft, Methodology, Conceptualization. **M. Milazzo:** Formal analysis. **O. Ruiz de Ballesteros:** Conceptualization. **M. Petrozziello:** Formal analysis. **A. Asproudi:** Formal analysis. **A. Carpignano:** Resources, Conceptualization. **R. Gerboni:** Writing – review & editing, Writing – original draft, Methodology, Conceptualization.

Declaration of competing interest

The authors declare that they have no known competing financial interests or personal relationships that could have appeared to influence the work reported in this paper.

Appendix A. Supplementary data

Supplementary data to this article can be found online at https://doi.org/10.1016/j.jclepro.2025.145003.

Data availability

Data will be made available on request.

References

Adesina, I., Bhowmik, A., Sharma, H., Shahbazi, A., 2020. A review on the current state of knowledge of growing conditions, agronomic soil health practices and utilities of hemp in the United States. Agriculture (Switzerland) 10 (Issue 4). https://doi.org/10.3390/agriculture10040129.

Agbo, P., Mali, A., Deng, D., Zhang, L., 2023. Bio-oil-based epoxy resins from thermochemical processing of sustainable resources: a short review. Journal of Composites Science 7 (9). https://doi.org/10.3390/jcs7090374.

Ares-Elejoste, P., Seoane-Rivero, R., Gandarias, I., Iturmendi, A., Gondra, K., 2023. Sustainable alternatives for the development of thermoset composites with low environmental impact. Polymers 15 (13), 2939. https://doi.org/10.3390/polym15132939.

Arpitha, G.R., Mohit, H., Madhu, P., Verma, A., 2024. Effect of sugarcane bagasse and alumina reinforcements on physical, mechanical, and thermal characteristics of epoxy composites using artificial neural networks and response surface methodology. Biomass Conv. Bioref. 14, 12539–12557. https://doi.org/10.1007/s13399-023-03886-7.

Auvergne, R., Caillol, S., David, G., Boutevin, B., Pascault, J.P., 2014. Biobased thermosetting epoxy: present and future. Chem. Rev. 114 (2), 1082–1115. https://doi.org/10.1021/cr3001274.

Balat, M., 2011. An overview of the properties and applications of biomass pyrolysis oils. Energy Sources, Part A Recovery, Util. Environ. Eff. 33 (7). https://doi.org/10.1080/15567030903228914.

Baroncini, E.A., Kumar Yadav, S., Palmese, G.R., Stanzione, J.F., 2016. Recent advances in bio-based epoxy resins and bio-based epoxy curing agents. J. Appl. Polym. Sci. 133 (45). https://doi.org/10.1002/app.44103. John Wiley and Sons Inc.

Bartoli, M., Duraccio, D., Faga, M.G., Piatti, E., Torsello, D., Ghigo, G., Malucelli, G., 2022. Mechanical, electrical, thermal and tribological behavior of epoxy resin composites reinforced with waste hemp-derived carbon fibers. J. Mater. Sci. 57 (31). https://doi.org/10.1007/s10853-022-07550-9.

Bartoli, M., Rosi, L., Giovannelli, A., Frediani, P., Frediani, M., 2020. Characterization of bio-oil and bio-char produced by low-temperature microwave-assisted pyrolysis of olive pruning residue using various absorbers. Waste Manag. Res. 38 (2). https://doi.org/10.1177/0734242X19865342.

Bhushan, B., 2013. Introdution to Tribology. John wiley & sons.

Bourne, L.B., Milner, F.J., Alberman, K.B., 1959. Health problems of epoxy resins and amine-curing agents. Br. J. Ind. Med. 16 (2). https://doi.org/10.1136/oem.16.2.81.

Brandrup, J., Immergut, E.H., 1975. Polymer Handbook, second ed.

Celikbag, Y., Meadows, S., Barde, M., Adhikari, S., Buschle-Diller, G., Auad, M.L., Via, B. K., 2017. Synthesis and characterization of bio-oil-based self-curing epoxy resin. Ind. Eng. Chem. Res. 56 (33). https://doi.org/10.1021/acs.iecr.7b02123.

Correa, C.E., Betancourt, S., Vázquez, A., Gañan, P., 2015. Wear resistance and friction behavior of thermoset matrix reinforced with Musaceae fiber bundles. Tribol. Int. 87. https://doi.org/10.1016/j.triboint.2015.02.015.

Delmastro, R.G.F., 2010. Sfibratrice Per Canapa Industriale.

Duque Schumacher, A.G., Pequito, S., Pazour, J., 2020. Industrial hemp fiber: a sustainable and economical alternative to cotton. J. Clean. Prod. 268. https://doi.org/10.1016/j.jclepro.2020.122180.

Finnan, J., Styles, D., 2013. Hemp: a more sustainable annual energy crop for climate and energy policy. Energy Policy 58. https://doi.org/10.1016/j.enpol.2013.02.046.

Flory, P., Rehner, J., 1943. Statistical mechanics of cross-linked polymer networks II. Swelling. J. Chem. Phys. 11, 521–526. https://doi.org/10.1063/1.1723792.

Foong, S.Y., Chan, Y.H., Cheah, W.Y., Kamaludin, N.H., Tengku Ibrahim, T.N.B., Sonne, C., Peng, W., Show, P.L., Lam, S.S., 2021. Progress in waste valorization using advanced pyrolysis techniques for hydrogen and gaseous fuel production. Bioresour. Technol. 320. https://doi.org/10.1016/j.biortech.2020.124299.

García, N., Compañ, V., Díaz-Calleja, R., Guzmán, J., Riande, E., 2000. Comparative study of the relaxation behaviour of acrylic polymers with flexible cyclic groups in their structure. Polymer 41 (17). https://doi.org/10.1016/S0032-3861(99)00889-7.

Ghodake, G.S., Shinde, S.K., Kadam, A.A., Saratale, R.G., Saratale, G.D., Kumar, M., Palem, R.R., AL-Shwaiman, H.A., Elgorban, A.M., Syed, A., Kim, D.Y., 2021. Review on biomass feedstocks, pyrolysis mechanism and physicochemical properties of biochar: state-of-the-art framework to speed up vision of circular bioeconomy. J. Clean. Prod. 297. https://doi.org/10.1016/j.jclepro.2021.126645.

Glinka, C.J., 2001. Methods of X-ray and neutron scattering in polymer science. Phys. Today 54 (3). https://doi.org/10.1063/1.4761820.

Hassan, E.B.M., Steele, P.H., Ingram, L., 2009. Characterization of fast pyrolysis bio-oils produced from pretreated pine wood. Appl. Biochem. Biotechnol. 154 (1–3). https://doi.org/10.1007/s12010-008-8445-3.

Heux, L., Halary, J.L., Lauprêtre, F., Monnerie, L., 1997. Dynamic mechanical and 13C n. m.r. investigations of molecular motions involved in the β relaxation of epoxy networks based on DGEBA and aliphatic amines. Polymer 38 (8). https://doi.org/10.1016/S0032-3861(96)00694-5.

Jiang, H., Cheng, Q., Jiang, C., Zhang, J., Yonghua, L., 2015. Effect of stick-slip on the scratch performance of polypropylene. Tribol. Int. 91. https://doi.org/10.1016/j.triboint.2015.06.024.

Kim, S., Lee, Y., Andrew Lin, K.Y., Hong, E., Kwon, E.E., Lee, J., 2020. The valorization of food waste via pyrolysis. J. Clean. Prod. 259. https://doi.org/10.1016/j.jclepro.2020.120816.

Koike, T., 2012. Progress in development of epoxy resin systems based on wood biomass in Japan. Polym. Eng. Sci. 52 (Issue 4). https://doi.org/10.1002/pen.23119.

Kousaalya, A., Iyer, R., Pilla, S., 2020. Eco-profiling of bio-epoxies via life cycle assessment. SAE J. STEEP 1, 39–57. https://doi.org/10.4271/13-01-01-0003.

Kumar, S., Adams, W.W., 1987. Structural studies of epoxy resins, acetylene terminated resins and polycarbonate. Polymer 28 (9). https://doi.org/10.1016/0032-3861(87)90349-1.

Li, C., Strachan, A., 2018. Cohesive energy density and solubility parameter evolution during the curing of thermoset. Polymer 135. https://doi.org/10.1016/j.polymer.2017.12.002.

Lindvig, T., Michelsen, M.L., Kontogeorgis, G.M., 2002. A Flory-Huggins model based on the Hansen solubility parameters. Fluid Phase Equilib. 203 (1–2). https://doi.org/10.1016/S0378-3812(02)00184-X.

Liu, S., Chevali, V.S., Xu, Z., Hui, D., Wang, H., 2018. A review of extending performance of epoxy resins using carbon nanomaterials. Compos. B Eng. 136. https://doi.org/10.1016/j.compositesb.2017.08.020.

Lovell, R., Windle, A.H., 1990. WAXS investigation of local structure in epoxy networks. Polymer 31 (4). https://doi.org/10.1016/0032-3861(90)90274-3.

Menezes, P.L., Kishore, Kailas, S.V., 2009. Influence of surface texture and roughness parameters on friction and transfer layer formation during sliding of aluminium pin on steel plate. Wear 267 (9–10). https://doi.org/10.1016/j.wear.2009.06.003.

Ning, S.K., Hung, M.C., Chang, Y.H., Wan, H.P., Lee, H.T., Shih, R.F., 2013. Benefit assessment of cost, energy, and environment for biomass pyrolysis oil. J. Clean. Prod. 59. https://doi.org/10.1016/j.jclepro.2013.06.042.

Pappa, C., Feghali, E., Vanbroekhoven, K., Triantafyllidis, K.S., 2022. Recent advances in epoxy resins and composites derived from lignin and related bio-oils. Curr. Opin. Green Sustainable Chem. 38. https://doi.org/10.1016/j.cogsc.2022.100687.

Pascoe S., Ortiz, 2023. Are bioplastics the solution to the plastic pollution problem? PLoS Biol. 21 (3), e3002045. https://doi.org/10.1371/journal.pbio.3002045.

Pulikkalparambil, H., Siengchin, S., Parameswaranpillai, J., 2018. Corrosion protective self-healing epoxy resin coatings based on inhibitor and polymeric healing agents encapsulated in organic and inorganic micro and nanocontainers. Nano-Structures and Nano-Objects 16. https://doi.org/10.1016/j.nanoso.2018.09.010.

Pupin, C., Ross, A., Dubois, C., Rietsch, J.C., Vernet, N., Ruiz, E., 2017. Formation and suppression of volatile-induced porosities in an RTM epoxy resin. Compos. Appl. Sci. Manuf. 94. https://doi.org/10.1016/j.compositesa.2016.12.006.

Rahul, R., Kitey, R., 2016. Effect of crosslinking on dynamic mechanical and fracture behavior of epoxy variants. Compos. B Eng. 85. https://doi.org/10.1016/j.compositesb.2015.09.017.

Raquez, J.M., Deléglise, M., Lacrampe, M.F., Krawczak, P., 2010. Thermosetting (bio) materials derived from renewable resources: a critical review. Prog. Polym. Sci. 35 (4). https://doi.org/10.1016/j.progpolymsci.2010.01.001.

Regulation (EU), 2024. 2024/1781 of the European parliament and of the council of 13 june 2024 establishing a framework for the setting of ecodesign requirements for sustainable products, amending directive (EU) 2020/1828 and regulation (EU) 2023/1542 and repealing directive 2009/125/EC. https://eur-lex.europa.eu/eli/reg/2024/1781/oj.

Rosenboom, J.G., Langer, R., Traverso, G., 2022. Bioplastics for a circular economy. Nat. Rev. Mater. 7, 117–137. https://doi.org/10.1038/s41578-021-00407-8.

Shahid, A.T., Silvestre, J.D., Hofmann, M., Garrido, M., Correia, J.R., 2024. Life cycle assessment of an innovative bio-based unsaturated polyester resin and its use in glass fibre reinforced bio-composites produced by vacuum infusion. J. Clean. Prod. 441, 140906. https://doi.org/10.1016/j.jclepro.2024.140906.

Sharath, B.N., Yashas Gowda, T.G., Madhu, P., Pradeep Kumar, C.B., Jain, N., Verma, A., Sanjay, M.R., Siengchin, S., 2024. Fabrication of raw and chemically treated biodegradable *Luffa aegyptica* fruit fibre-based hybrid epoxy composite: a mechanical and morphological investigation. Biomass Conv. Bioref. https://doi.org/10.1007/s13399-024-05570-w.

Zakaria, M.Y., Sulong, A.B., Sahari, J., Suherman, H., 2015. Effect of the addition of milled carbon fiber as a secondary filler on the electrical conductivity of graphite/epoxy composites for electrical conductive material. Compos. B Eng. 83. https://doi.org/10.1016/j.compositesb.2015.08.034.

Zhang, S.Y., Ding, Y.F., Li, S.J., Luo, X.W., Zhou, W.F., 2002. Effect of polymeric structure on the corrosion protection of epoxy coatings. Corros. Sci. 44 (4). https://doi.org/10.1016/S0010-938X(01)00091-9.

Zhang, Y., Fan, X., Zhang, Z., Si, C., Li, T., Zhu, M., 2024a. PSF@ PAO40 microcapsules enhanced epoxy resin coating toward anti-wear/corrosion performance. Colloids Surf. A Physicochem. Eng. Asp. 700, 134828. https://doi.org/10.1016/j.colsurfa.2024.134828.

Zhang, Y., Si, C., Zhang, Z., Li, L., Fan, X., Zhu, M., 2024b. b. Hierarchical design of microcapsules-based epoxy resin coating enhanced with Ti3C2Tx for improving thermal, tribological, anti-corrosive performance. Carbon 228. https://doi.org/10.1016/j.carbon.2024.119379.

Zimniewska, M., 2022. Hemp fibre properties and processing target textile: a review. Materials 15 (Issue 5). https://doi.org/10.3390/ma15051901.

Zong, P., Jiang, Y., Tian, Y., Li, J., Yuan, M., Ji, Y., Chen, M., Li, D., Qiao, Y., 2020. Pyrolysis behavior and product distributions of biomass six group components: starch, cellulose, hemicellulose, lignin, protein and oil. Energy Convers. Manag. 216. https://doi.org/10.1016/j.enconman.2020.112777.